Neural Computing and Applications (2025) 37:8273–8284
https://doi.org/10.1007/s00521-025-11006-x

ORIGINAL ARTICLE

FedLRes: enhancing lung cancer detection using federated learning with convolution neural network (ResNet50)

C. Usharani[1] · A. Selvapandian[2]

Received: 9 August 2024 / Accepted: 10 January 2025 / Published online: 3 February 2025

Abstract

Lung cancer remains a leading global cause of mortality, necessitating efficient early detection. Lung cancer image analysis plays a pivotal role, yet current manual segmentation by oncologists is laborious. Our innovative (FedLRes) approach proposes a comprehensive system for automated diagnoses of lung cancer using federated learning with ResNet50. The lung cancer dataset from the Iraq-Oncology Teaching Hospital/National Centre for Cancer Diseases was gathered by the IQ-OTH/NCCD. The dataset consists of 1097 images, split into training (822 images) and validation (275 images) sets. The training set includes 312 normal, 420 malignant, and 90 benign cases. The training set's data are further enhanced by using data augmentation techniques, which are then applied to normalise images differences before being fed into the federated learning with ResNet50 architecture. This approach combines deep learning models trained on different datasets allowing for improvising accuracy and generalisation. The federated learning approach enables the use of distributed data while ensuring data privacy and security. The proposed approach compared with different state of art algorithms. Through rigorous experimentation, our system showcases remarkable advancements a classification accuracy of 99.40%. This innovative approach, utilising 3D input CT scan data, offers a potent and precise tool for early detection and effective treatment strategies against the scourge of lung cancer.

Keywords Image processing · Lung cancer · Federated learning · ResNet50 · Augmentation

1 Introduction

Lung cancer will be the cause of 22, 06, 771 new cases and 17, 96, 144 deaths in 2020, according to GLOBOCAN. The most frequent cancer in males and the third most prevalent in women is lung cancer. In India, with 72, 510 cases and 66, 279 fatalities, it is the fourth most frequent cancer. It is responsible for a startling 18.0% of cancer-related fatalities as well as 11.4% of newly diagnosed instances of the disease [1]. Lung cancer is recognised as one of the deadliest and most dangerous forms of cancer. Apart from the fact, the survival rate following a late diagnosis is dismal, sometimes virtually non-existent. This deadly disease is caused by malignant cells growing out of control in one or both lungs, and it is harmful because those cells can migrate to other parts of the body.

On the other hand, because of gene promoter methylation, sputum has sufficient capacity to identify lung cancer in its early stages; however, further research was required [2]. Additionally, VOC in urine had good specificity and sensitivity but needed a larger sample size for the research, whereas CXR has low sensitivity and a high percentage of false-negative results [3, 4]. These days, computed tomography (CT) imaging, which provides precise information about the positions and sizes of nodules, is the most effective method for detecting lung cancer. Early cancer detection of the tumours was made possible by the low-dose CT screening. When compared to conventional radiography procedures, it led to a 20.0% decrease in mortality and a significant rise in the rate of positive screening tests [5].

✉ C. Usharani
cusha91@gmail.com

A. Selvapandian
selvapandian.psna@gmail.com

[1] Department of Artificial Intelligence and Data Science, Ramco Institute of Technology, Rajapalayam, India

[2] Department of Electronics and Communication Engineering, Gnanamani College of Technology, Namakkal, India

The medical professionals and radiologist are facing the issue of identify the malignant cell because of the variations in CT scan image intensity and incorrect anatomical structure [6]. Computer-Aided Diagnosis tool will help doctors and radiologists effectively diagnose cancer. Numerous systems have been created, and research on lung cancer detection is ongoing. Most of the research community are working for the improvement to reach the maximum accuracy possible, which is close to 100%, while some systems do not have detection accuracy that is good enough. Thus far, the new artificial intelligence system has been successful in detecting 97% of tumours, which can aid in the early identification of lung cancer [7]. Lung cancer has been detected and classified with the use of ML and DL techniques. Initially, the researchers gave the machine learning approaches with data from the medical images [8].

M.F. Abdullah et al. used the KNN classifier algorithm for the lung cancer image classification with 85.5% accuracy. The main goal of this work is to design an image processing by the median filter-based pre-processing, feature extraction, and lung cancer classification using KNN [9]. Taher et al. used segmentation results for a Computer-Aided Diagnosis (CAD) system that will increase the patient's chances of survival by detecting lung cancer early it achieves the 98% accuracy.

Dandil et al. [10] used ANN for improve the accuracy of 90.63%. Using a neural network model of Self-Organising Maps (SOM), the developed CAD system segments lobe nodules and uses an artificial neural network (ANN) to classify nodules as benign or cancerous. Using 128 CT images from 47 patients in total, the CAD system demonstrated performance values of 90.63% accuracy, 92.30% sensitivity, and 89.47% specificity. Diaz et al. [11] used an artificial neural network and a genetic approach to choose features (genes) for the support vector machine and identify a patient's lung cancer status. Genes that characterise a patient's lung cancer status have been effectively found using genetic algorithms (GA) with remarkable prediction ability of 84% accuracy. Zheng et al. [12] used convolution neural network for the lung cancer analysis using CNN and achieve the accuracy of 94.61%.

Yasriy et al. used three preparation steps such as feature extraction techniques, image segmentation, and image enhancement. Finally, the instances on the slides are classified as belonging to one of the three classes using support vector machine (SVM) as a classification approach. These classifications are normal, benign, or malignant. Various SVM kernels and methods for extracting features are assessed. About 89.8876% was the highest accuracy attained using this approach on the newly created dataset [13]. The same author used CNN in this dataset and achieves the 93.54% accuracy in this dataset [14].

Using an active contour model and fuzzy interference system, Roy, Sirohi, and Patle [15] created a method to identify lung cancer nodules. Grey transformation is used by this technology to improve the contrast of images. Cases of cancer are categorised using the fuzzy inference method. The total accuracy of the system is 94.12%. Using two distinct residual convolutional blocks, Fuli Zhang et al. [16] exploited the deep features of the computed tomography images, combining the features from each ResNet level into a single output. This simple method merged deep semantic data with superficial appearance criteria to produce dense pixel outputs.

Nakrani et al. [17] suggested method segments the lungs using morphological operations and detects lung nodules using a convolutional neural network. The purpose of this approach is to lessen radiologists' burden by giving them a second viewpoint. A total of 1010 CT patients' chest area images were obtained for testing using the LIDC (Lung Image Database Consortium) collection. On the test dataset, the model was able to get top-5 accuracy of 95.24%. CBAM-ResNet performs better by integrating the clinical data with the morphological characteristics (AUC: 0.957 and accuracy: 0.898). By contrast, the accuracy and AUC values of a radiomic analysis that employed NSDTCT-SVM were 0.779 and 0.807, respectively. Zhang et al. [18] used a multi-view knowledge-based collaborative (MV-KBC) deep model to discriminate between benign and malignant lung nodules. This approach has an accuracy and an AUC of 91.60% and 95.70%, respectively.

In order to differentiate between benign and malignant pulmonary nodules, Xie et al. [19, 20] developed a method dubbed Fuse-TSD that incorporated texture, shape, and deep model-learnt information. Three AdaBoosted BPNNs were trained using the three different feature types, and the classifiers' outputs were combined to classify the nodules. On the LIDC-IDRI dataset, the suggested technique was claimed to achieve an AUC of 96.65%, 94.45%, and 81.24%.

The computers then follow an algorithm or set of instructions to learn how to recognise patterns linked to each ailment and diagnose the specific type of illness. In this field, minimising misclassification errors is a significant difficulty. In order to overcome misclassification mistakes, we have proposed a federated learning-based approach in this study. This is a novel approach in the domain of classification.

The main objectives of this article are highlighted as follows:

1. Load the data into the server. The data can be distributed to the client, and ResNet50 architecture is executed separately in each client.

2. Each client generates the weight according to the correct classification. All the weights are transferred to the server.
3. The server build its own architecture based on the weight generated by clients with the averaging techniques.
4. The classification can be carried out based on the model build by the server.

The rest of the paper is organised in this manner. Section 2 discusses the relevant works. The procedures for gathering the data and analysing it by using federated learning with Resnet50 architecture for accurately diagnose lung cancer from CT images. The conclusion and future directions are covered in Sect. 3. Many techniques, including transfer learning, re-enforcement learning, and meta-learning, have been proposed by researchers in the field of deep learning-based image categorisation.

2 Methodology

This section provides the specifics of our suggested approach for classifying lung cancer image classification. The approach comprises the subsequent stages: (i) gathering and enhancing data; (ii) utilising the ResNet architecture for federated learning; (iii) outlining our recommended framework; and (iv) explaining the client-side and server-side model aggregation procedures. Figure 1 portrays the overall architecture of the proposed model. Biological neural networks serve as the model for artificial neural networks or neural networks (NNs), which are computer systems built around an artificial neuron, which is a collection of interconnected processing units (nodes). Compared to previous machine learning (ML) techniques, they have demonstrated superior outcomes and revolutionised nearly all medical sectors [21–23]. It has been demonstrated that a neural network could converge on any dataset with just two hidden layers of nodes. In the context of image processing, the term "deep learning" (DL) refers to networks with a higher number of intermediate layers.

Typically, these networks have a few convolutional layers. These layers create feature maps, or translation-equivalent responses, by sliding kernels, also known as filters, along input features. By changing parts of the current layers—typically the last ones—and maintaining the remaining layers with their weights, transfer learning [24–26] refers to the process of adapting a network that was trained for one task to another. The federated learning [27–29] based deep learning algorithms plays a major role image classification, and the outcomes are typically more favourable. Here, we proposed FedLRes framework, and it produces the 99.6% accuracy which is better compare to other classifier algorithm.

Our method, FedLRes, offers a new and all-inclusive methodology for automated lung cancer diagnosis. We

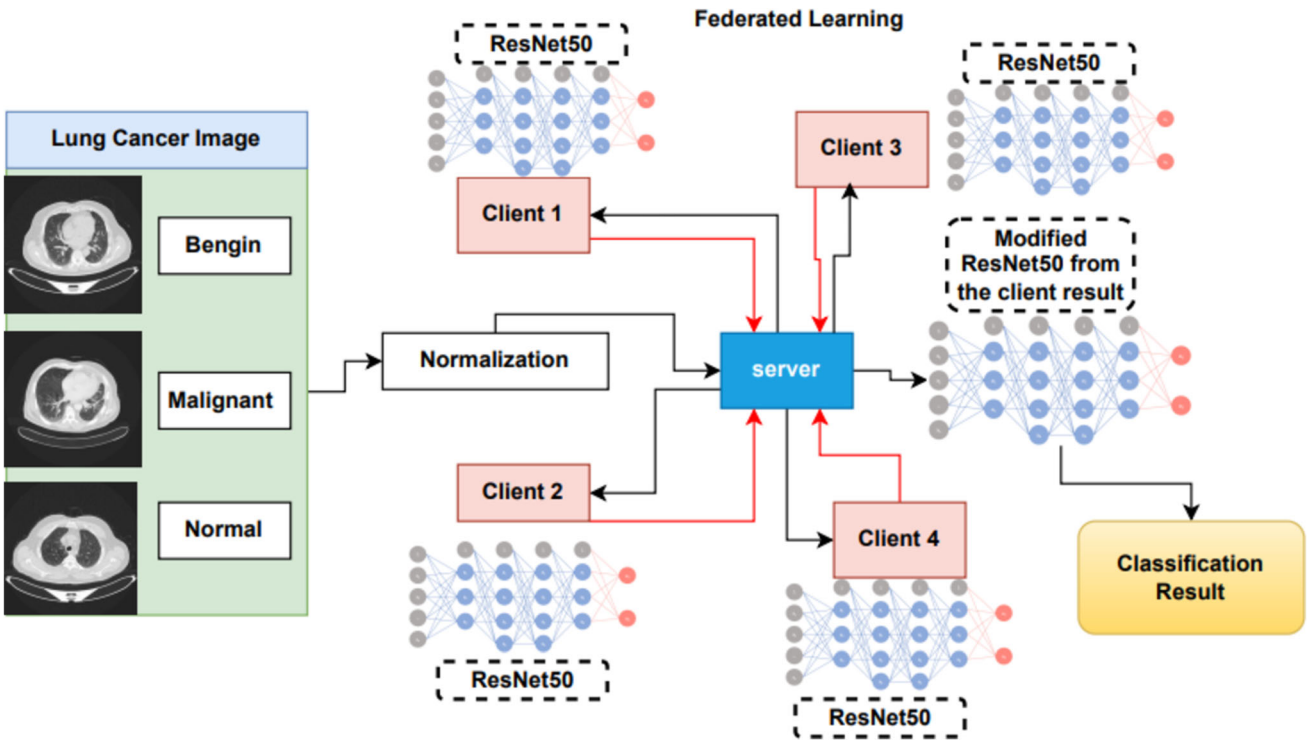

Fig. 1 FedLRes framework for lung cancer analysis from CT scan image

enable collaborative learning from decentralised data sources while maintaining data privacy by utilising federated learning in conjunction with the robust ResNet50 architecture. By combining the deep learning algorithm with federated learning, this innovation seeks to improve the precision and effectiveness of lung cancer detection from images.

2.1 Data collection and pre-processing

The CT scan images for lung cancer used in this investigation were taken from the publically accessible (IQ-OTH/NCCD) [13, 27–34] dataset. In the final quarter of 2019, the dataset was collected at two specialised hospitals located in Iraq. The dataset's main objective is to categorise individuals into one of three lung cancer modalities, which are selected by oncologists and radiologists: benign (BGN), malignant (MLG), or normal (NRM). A total of 1190 images in all, representing CT scan slices of 110 instances, are included in the collection. The three groups of these instances are malignant, benign, and normal. Thirty-five of them have been classified as benign, forty as malignant, and forty as normal. At first, DICOM format was used to collect the CT images. The scanner used is a Siemens SOMATOM model. After every photo was de-identified, analyses were carried out. The oversight review board decided not to require written consent. The collaborating medical centres' institutional review boards authorised the study. Every scan has many slices. These slices come in an assortment of 80–200 pieces, each of which depicts a distinct side and angle of a human chest. The 110 cases differ in terms of living situation, location of residence, age, gender, and level of education. A portion of them work for the Iraqi ministries of oil and transportation, while others are gainers and farmers. The majority of them are from Iraq's middle area, specifically the provinces of Babylon, Wasit, Diyala, Salahuddin, and Baghdad. The sample images are listed here.

2.2 Federated learning for classification

One type of distributed learning approach is federated learning. The core model is distributed to several user terminals and is maintained on the server. Users build learning models on local terminals to address privacy concerns. The server will extract the user terminal in accordance with the proportion and set the score S in order to update the server's central model. Next, update the server model parameters by uploading the user-improved model parameters.

The environment of this federated learning setup is made to include several clients, all of whom take part in decentralised model training. Four clients make up the system, and each one works with a locally distributed subset of the data to prevent clients from sharing raw data. Because each client only views and trains on its own data, not the complete dataset, this partitioned data preserves privacy. Using local data, the clients autonomously train their local models, modifying the model weights according to their unique datasets. Each client uses a local optimiser to update its model parameters and compute the gradients during the course of the training process, which spans several epochs. The client model parameters are combined into a global model after each client's local training is finished. In order to ensure that each client's contribution is represented in the global model update, this aggregation usually entails averaging the weights of the models from all clients. After every epoch, the global model is updated repeatedly, with each client making incremental improvements to the global model.

The user terminal model is then improved by sending it to user terminals. In this way, we continuously improve both the server's central model and the user terminal's local model. Federated learning (FL) emerges as a transformative approach in machine learning, offering a solution to privacy concerns while harnessing the collective intelligence of decentralised data sources. This methodology allows for the collaborative training of a ResNet 50 across multiple client devices or servers, all while ensuring that sensitive raw data remain within the confines of the local environment [35, 36].

To solve the issue of disappearing gradients in deep neural networks, ResNet50 adds residual blocks. Within the architecture, a residual block is a construction block that facilitates information flow via shortcut connections. These connections allow the gradient to bypass certain layers during backpropagation, mitigating the diminishing gradient issue and facilitating the training of very deep networks. ResNet50 is a deep convolutional neural network with skip connections, making it suitable for feature extraction in image-related tasks. Here, X as the imput image, F_i as the features at layer i, w_i as the weights of layer i, b_i as the bias term of layer i, and σ as the activation function. ResNet50 is a deep CNN with skip connections, making it suitable for feature extraction in image-related tasks [37, 38].

Particularly advantageous for applications involving confidential data, such as healthcare and finance, FL ensures both privacy compliance and enhanced model performance. Incorporating ResNet50 into federated learning involves adapting the ResNet50 architecture for decentralised model training across multiple clients. ResNet50, known for its effectiveness in training deep neural networks, can be customised for federated scenarios where each client contributes to the global model's improvement.

Initially, a CNN model, such as ResNet50, is loaded either pretrained or with random weights. To tailor ResNet for federated settings, a custom Client ResNet50 model is defined, inheriting from ResNet and modified for local client training. This custom model includes an added fully connected layer adapted for the specific classification task, denoted as $f_{client}(x; \varnothing_c)$, where x represents the input data, and $\varnothing_c$ is the model parameters.

$$f_{\text{client}}(x; \varnothing_c) = ResNet(x; \varnothing_c)$$

The ResNet50 architecture is discussed in Table 1.

During local training on each client's dataset, the model optimises its parameter $\varnothing_c$ using SGD with the cross-entropy loss £. The local training loop minimises the loss between predicted outputs $\overline{y}$ and true labels y, updating the model parameters via backpropagation:

$$£(\overline{y}, y) = -\sum_{c=1}^{C} y_c \log(\overline{y_c})$$

$$\emptyset_c^{(t+1)} = \emptyset_c^{(t)} - €\nabla £\left(\overline{y}, y; \emptyset_c^{(t)}\right)$$

Here, € represents the learning rate, $\overline{y_c}$ is the predicted probability for class c, and y_c is the true label for class c. Each client model, $f_{client}(x; \varnothing_c)$, undergoes local training for a specified number of epochs. The local training is performed over a mini-batch of data, updating the model parameters as follows:

$$\emptyset_c^{(t+1)} = \emptyset_c^{(t)} - €\frac{1}{|\infty|}\sum_{(x,y)\in\infty} \nabla £\left(f_{\text{client}}\left(x; \emptyset_c^{(t)}\right), y\right)$$

Here, ∞ represents the mini-batch of data, $|\infty|$ is the batch size, and $\nabla £(f_{\text{client}}\left(x; \varnothing_c^{(t)}\right), y)$ is the gradient of the loss with respect to the more parameters.

After local training, the updated client model's weights are aggregated to form a new global model (ResNet) $f_{\text{global}}(x; \varnothing_g)$. The gloabal model is updated by averaging the weights of the client models:

$$\varnothing_g^{(t+1)} = \frac{1}{N}\sum_{c=1}^{N} \varnothing_c^{(t+1)}$$

Here, N represents the total number of clients in the federated systems. This aggregation step ensures that the global model reflects an amalgamation of the insights learnt from each client's local dataset while maintaining privacy and decentralisation.

The federated learning process iterates through multiple global epochs, where each epoch consists of local training on all client datasets followed by aggregation of model updates. This iterative process fosters collaborative learning across distributed datasets without sharing raw data. The model can successfully exploit the collective knowledge from multiple datasets while maintaining data privacy and security by modifying the ResNet50 architecture inside this federated framework. This makes the model appropriate for use in sensitive sectors such as finance and healthcare.

Cross-entropy was the loss function used to each entity in the ResNet50 models. A loss function called cross-entropy is used to gauge how well a classification model is working. The cross-entropy function becomes binary cross-entropy in applications with two classes. The suggested approach, however, uses a multiclass categorisation. As a result, a different loss was computed for each label and observation in order to determine the loss of each model for each entity deployed. The following equation calculated the total loss for every entity that participated in the training and validation process by adding together all of the losses for each label. If y was the binary value showing

Table 1 ResNet50 architecture

Layer Type	Output Shape	Kernel Size	Stride	Filters/Channels
Input Layer	(224, 224, 3)	–	–	–
Conv1	(112, 112, 64)	7 × 7	2	64
Max Pooling	(56, 56, 64)	3 × 3	2	–
Residual Block 1 (× 3)	(56, 56, 64)	3 × 3	1	64
Residual Block 2 (× 4)	(28, 28, 128)	3 × 3	2	128
Residual Block 3 (× 6)	(14, 14, 256)	3 × 3	2	256
Residual Block 4 (× 3)	(7, 7, 512)	3 × 3	2	512
Average Pooling	(1, 1, 512)	7 × 7	1	–
Fully Connected (FC)	(1, 1, 1000)	–	–	1000 (output)
Softmax Activation	(1, 1000)	–	–	–

whether observation o was correctly categorising the label i, p was the number of classes, and L was the

$$\text{Loss} = \sum_{i=1}^{L} y_{o,i} \log(P_{o,i})$$

The key equations for federated learning with ResNet include the loss function £, SGD parameter updates, and the aggregation of client model weights to update the global model [39–41]. These equations form the backbone of the decentralised training process, enabling collaborative model improvement across distributed data sources. The steps for the federated learning architecture for lung cancer detection from CT images are depicted in Fig. 2.

- **Step 1:** Carries out task initiation. The training job, which is to identify the target application and the associated data needs, is determined by the server. In addition, throughout the training process, the server sets parameters like the learning rate and defines the global model. Afterwards, the server allocates the initialised global model g_m and training tasks to the participating clients to complete the task allocation. It initialises the weights wi^{t-1}, and it shared with a subset of clients.
- **Step 2:** Performs the training and upgrading of the local model. Using local data and equipment, each participating user changes the local model parameters based on the global model $g_m(t)$, where t is the current iteration index. Each client receives the weight parameters from step 1 and performs the training steps on a mini-batch b with a local objective function F_k and local learning rate ϵ_{local}. Here, it uses the stochastic gradient descent optimiser for optimise the parameters.
- **Step 3:** Acknowledging the compilation and modernisation of the worldwide model. The users who have the data are sent the updated global model parameters by the server, which has aggregated the local models of all participating users.

Here, four clients are participated in the federated learning. Each client is having all the same ResNet architecture and loss function. It is listed in Algorithm 1. The client computes a gradient update to create a new updated model that is shared with the aggregation server after performing SGD iterations as many times as the number of local epochs.

Algorithm 1: Client-side update

Input: Learning Rate α, loss function σ, no of epochs and local training data

Function ClientWeights(wc_t)

$wc = wc_t$

B = split L_k into batches of size B

For each epoch (i)in local machine up to E

For each batch (b) in B do

Compute gradient gr_i^b for each batch b by ∇ σ(wc; $batch$)

Update local model $wc = wc - \alpha gr_i^b$

End for

End for

End function

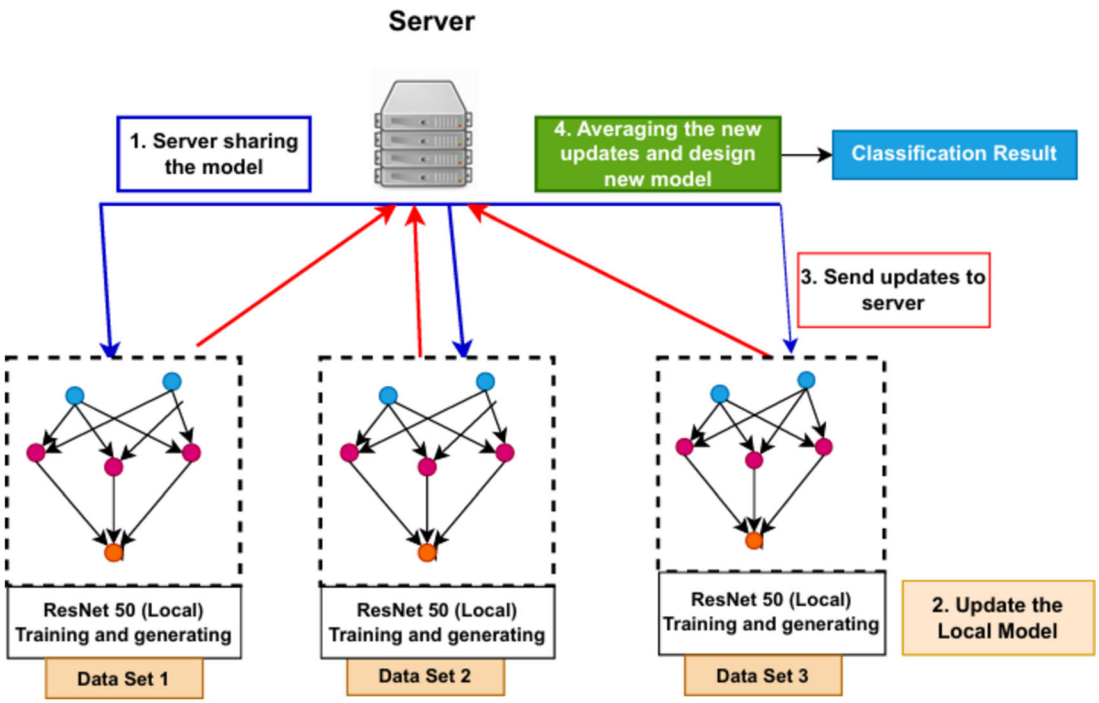

Fig. 2 Federated learning architecture for lung cancer detection from CT images

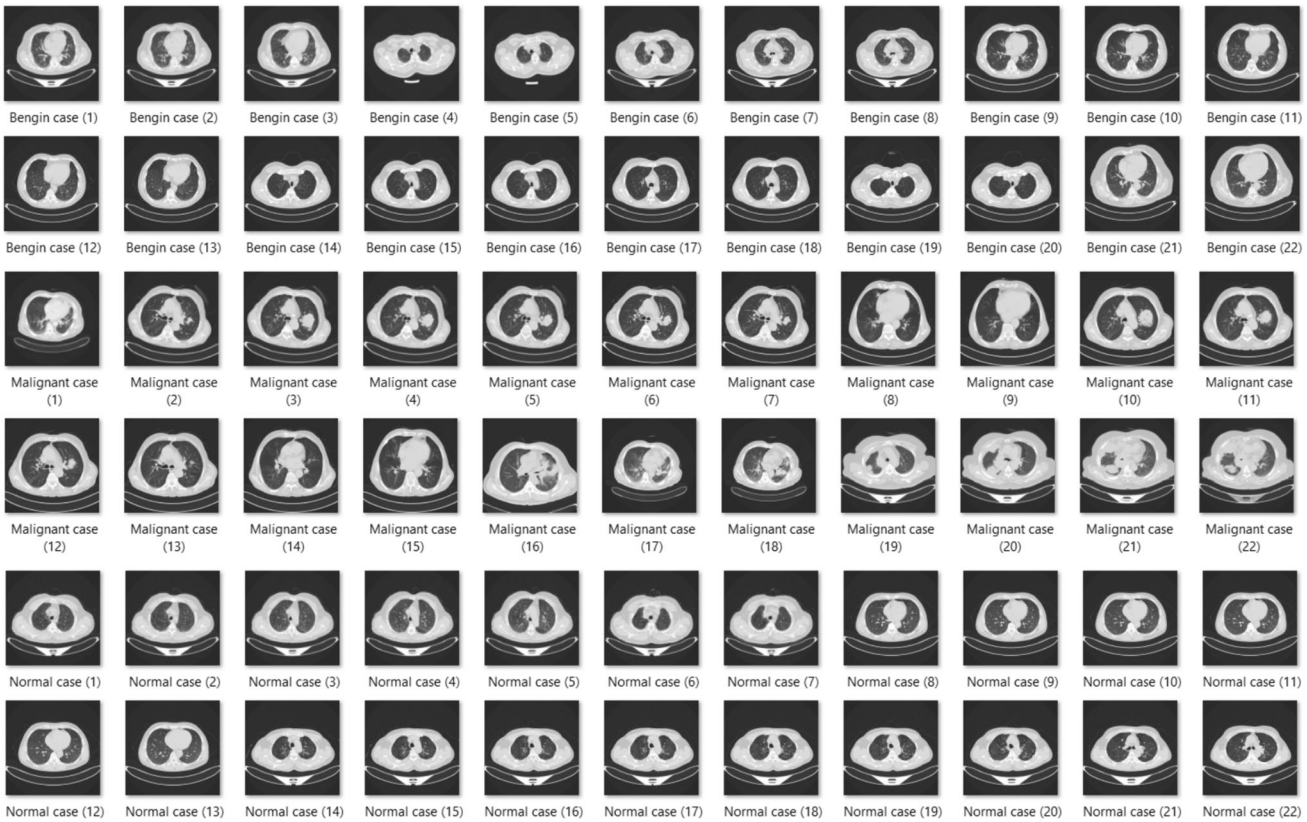

Fig. 3 Sample dataset

Table 2 Sample images used for training and validation

Number of images in training set: 822	Number of images in validation set: 275
Benign cases: 90 images	Benign cases: 30 images
Malignant cases: 420 images	Malignant cases: 141 images
Normal cases: 312 images	Normal cases: 104 images

The server that manages the global model and keeps track of the whole model training process provides the original model to each participating client. Updates are synchronised and received from all clients involved. The server-side aggregation process is depicted in Algorithm 2.

Algorithm 2: Server-side aggregation procedure

Input: Num_federated_rounds

Function Aggregate (cl, k)

Initialize the global model

For each round

$M = max(clXk, 1)$

s_t = (random set of m clients)

For each client $k \in s_t$ do

Send w^{t-1} to client k

$w_k^i = Client\ weight(k, w^{t-1})$

End for

$w^t = \sum_{k=1}^{k} \frac{n_k}{n} w_k^i$

End for

Return w^t

End function

It is possible to define two groups of parameters for the suggested approach. The parameters set for every ResNet50 DL model that is installed on a client serve as a representation of the first category. The values generated by the loss function during DL model training indicate whether or not a model is converging. The DL model optimiser uses these numbers to determine which weights need to be updated. Adam was selected as the optimiser for the suggested model. The stochastic gradient descent (SGD) technique serves as the foundation for the Adam optimiser. Adam, on the other hand, employed a different learning rate for every parameter than SGD, which maintains a consistent learning rate for every weight update.

The federated learning process iterates through multiple global epochs, where each epoch consists of local training on all client datasets followed by aggregation of model updates. This iterative process fosters collaborative learning across distributed datasets without sharing raw data. The model can successfully exploit the collective knowledge from multiple datasets while maintaining data privacy and security by modifying the ResNet50 architecture inside this federated framework. This makes the model appropriate for use in sensitive sectors such as finance and healthcare.

2.3 Results and discussion

The lung cancer dataset was collected over the course of 3 months in fall 2019 at the aforementioned specialised institutions by the Iraq-Oncology Teaching Hospital/National Centre for Cancer Diseases (IQ-OTH/NCCD). It includes CT images from both healthy people and patients who have had lung cancer at different stages of the disease. Oncologists and radiologists annotated IQ-OTH/NCCD slides at these two centres. The study's sample dataset is depicted in Fig. 3. Table 2 displays the sample training and validation count.

A total of 1097 images in all, split into training and validation sets, make up the dataset used in this investigation. The 822 images in the training set are then divided into three classes: 312 normal cases, 420 malignant cases, and 90 benign instances. There are 275 images in the validation set, comprising 104 normal cases, 141 cancer cases, and 30 benign ones. To provide transparency in the dataset production process, the selection methodology and curation of these photos should be explained in detail. This includes describing how the data were labelled, if it was balanced across various populations, and whether it came from a particular medical facility. It is also important to resolve any potential biases in the collection, including an imbalance in the number of photographs per class or in the representation of certain demographics. For example, there are much more malignant instances than benign and normal cases, which may cause class imbalance and affect the model's performance. The representativeness of the dataset and its suitability for training an objective, generalised model can be assessed by giving further details on the curation procedure and the reasoning for dataset division.

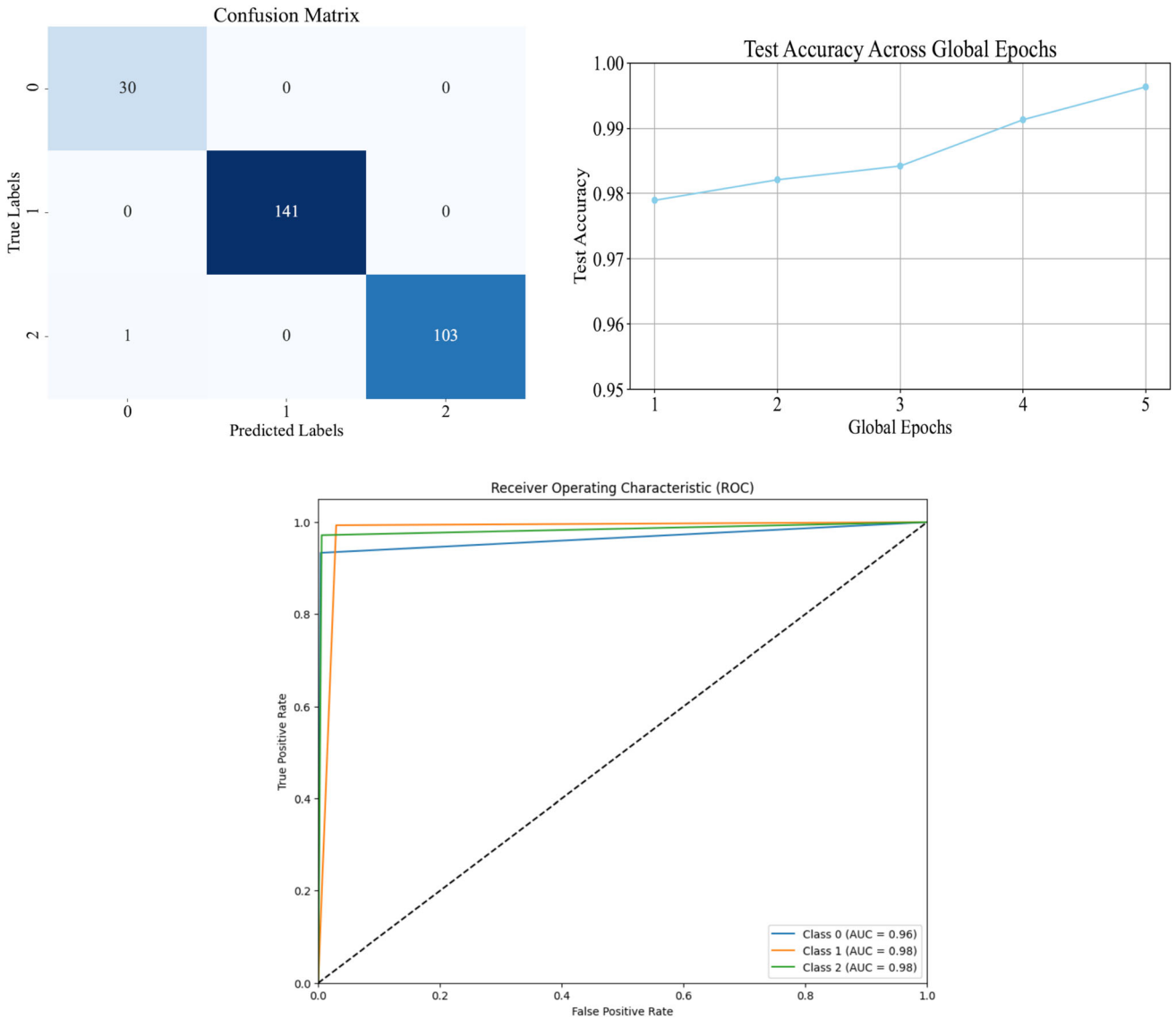

Fig. 4 **a** Confusion matrix. **b** Test accuracy across global epochs. **c** ROC curve

Table 3 Comparative analysis of the proposed algorithm with existing algorithm

Method	Accuracy	Sensitivity	Specificity	Precision
CNN optimised and improved Snake optimisation algorithm	96.58	95.38	94.08	84.16
KNN	85.25	85.32	83.32	71.09
CFM	87.24	87.24	86.65	75.94
WSDL	89.26	89.16	88.46	78.26
CLFM	92.46	91.08	90.39	81.39
DFD-Net	94.52	93.65	92.46	83.5
Proposed Model	99.40	99.03	99.36	98.92

Accuracy is a frequently used parameter in classification performance assessment that expresses the ratio of successfully categorised cases to all examined examples. The accuracy_score function, a vital component of the sklearn. metrics module, calculates the degree to which a machine learning model predicts future results. The accuracy (Acc) in mathematics is defined as follows:

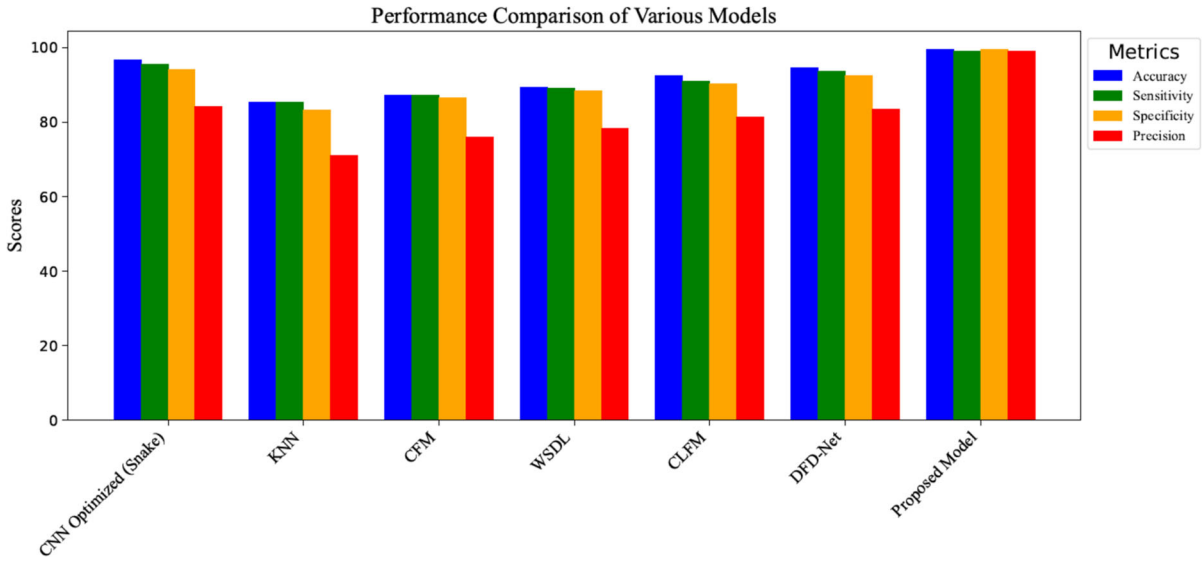

Fig. 5 Comparison chart for the proposed model

$$\text{Acc} = \frac{\text{TP} + \text{TN}}{\text{TP} + \text{TN} + \text{FP} + \text{FN}}$$

Another popular performance metric for assessing the effectiveness of machine learning models is the F1 score, which is especially useful when assessing the models' performance in binary classification tasks. It serves as an equalising element, balancing recall and precision to provide a single measurement that includes both sides. The F1 score has the following mathematical definition:

$$F1 = 2 \times \frac{\text{precision} \times \text{recall}}{\text{precision} + \text{recall}}$$

$$\text{precision} = \frac{\text{TP}}{\text{TP} + \text{FP}}$$

$$\text{recall} = \frac{\text{TP}}{\text{TP} + \text{FN}}$$

The F1 score is a numerical range that runs from 0 to 1. The ideal score is 1, which indicates perfect recall and precision. An elevated F1 score suggests a better overall model performance by indicating a fairer balance between precision and recall. Furthermore, by penalising models that place an excessive emphasis on recall or accuracy, the F1 score makes it possible to assess a model's capacity to provide accurate positive predictions while minimising the exclusion of genuine positive cases. When assessing machine learning modules, particularly those that carry out binary classification, the Area Under the Curve (AUC) and the Receiver Operating Characteristic (ROC) curve are essential measures. The ROC curve provides a visual representation of the connection between the true-positive rate (TPR) and false-positive rate (FPR) at various classification thresholds, which facilitates a deeper understanding of the sensitivity–specificity trade-off. The resultant scalar value, known as the AUC, is derived from the ROC curve and indicates the model's overall capacity for discrimination.

A key instrument for evaluating a classification model's effectiveness is the confusion matrix. It gives practitioners information about the advantages and disadvantages of the model, enabling them to choose and optimise it with knowledge. It is especially helpful in scenarios when the ramifications of false positives and false negatives differ. Figure shows the test accuracy throughout the worldwide epochs. Plotting the true-positive rate versus the false-positive rate yields the receiver operating characteristic curve graph, which is used to assess the efficacy of the proposed model and illustrates the system's ability to categorise data. The Area Under the Curve (AUC), which evaluates the overall quality of the model, is another statistic that may be seen on the ROC plot. The accuracy measure, ROC curve, and confusion matrix are shown in Fig. 4.

Several cutting-edge techniques are applied to improve model performance in lung cancer detection. By combining CNNs for feature extraction with the Snake Algorithm for tumour boundary refinement, the CNN Optimised and Improved Snake Optimisation Algorithm increases accuracy. Using a straightforward method, K-Nearest Neighbours (KNN) compares images to their nearest neighbours using features that have been retrieved. To handle complicated picture data, the Classification Forest Model (CFM), an ensemble approach, combines several decision trees to increase accuracy. Wavelet-based Spatial Discriminative Learning (WSDL) helps detect tumours in their early stages by capturing multi-scale data using wavelet transforms. The Cascaded Learning Framework (CLFM)

models lung cancer at different stages using a progressive, multi-phase methodology. Lastly, in order to differentiate between malignant and healthy tissues, the Deep Feature Discrimination Network (DFD-Net) concentrates on extracting discriminative features. The results of the recommended process are compared with those of the other aforementioned approaches in the next phase to determine its efficiency. The results of the comparison are shown in Table 3. Regarding Table 3, the best confirmation with the true data is provided by the suggested approach with 99.40% accuracy, which offers just a 98.92% precision. Additionally, the suggested method's 99.36% specificity, the greatest number among the other techniques under study, demonstrates the method's greater percentage of true negative, which characterises its capacity to diagnose non-tumour pixels accurately (Fig. 5).

3 Conclusion

Ultimately, our research addresses the urgent need for effective early diagnosis amid this difficult global health crisis, marking a substantial progress in the detection and categorisation of lung cancer. Our unique method, which combines adaptive feature optimisation with federated learning, allows for automated CT scan categorisation, giving oncologists quick and reliable information for diagnosis and treatment planning. We obtained an astounding 99.40% classification accuracy using the IQ-OTH/NCCD lung cancer dataset and an ensemble federated learning-based technique using ResNet50 for multi-order lung cancer classification. This outcome shows how effective our method is and represents a major advancement over traditional deep learning and machine learning methods. Given that federated learning preserves security and privacy while enabling the use of distant data, further research and use of this technology appear promising. Ultimately, our research significantly advances the ongoing battle against lung cancer by offering a reliable and precise response that might lead to more effective treatment regimens and, ultimately, improved patient outcomes.

Acknowledgements The authors would like to thank the supervisor for their valuable assistance in implementation work.

Authors' contribution The corresponding author of C. Usharani conceived and designed the study and performed experiments and analysed the data and wrote the paper.

Funding The authors declare that this research work does not have any funding agency.

Data availability The data and materials supporting the findings of this study are available upon data openly available in a public repository of the IQ-OTH/NCCD lung cancer that does not issue DOIs (https://www.kaggle.com/datasets/hamdallak/the-iqothnccd-lung-cancer-dataset).

Declarations

Conflict of interest The authors declare that they have no competing interests relevant to this research. I am C. Usharani, the corresponding author of this work of Enhancing Ling cancer detection using federated learning with convolution neural network (ResNet50). I certify that there is no actual or potential conflict of interest in relation to this article.

References

1. World Health Organization. Global Cancer Observatory-GLOBOCAN 2020. Available online: https://gco.iarc.fr. Accessed 16 Apr 2022
2. Belinsky SA, Klinge DM, Dekker JD, Smith MW, Bocklage TJ, Gilliland FD, Crowell RE, Karp DD, Stidley CA, Picchi MA (2005) Gene promoter methylation in plasma and sputum increases with lung cancer risk. Clin Cancer Res 11(18):6505–6511
3. Doria-Rose VP, Marcus PM, Szabo E, Tockman MS, Melamed MR, Prorok PC (2009) Randomized controlled trials of the efficacy of lung cancer screening by sputum cytology revisited: a combined mortality analysis from the Johns Hopkins lung project and the Memorial Sloan-Kettering lung study. Cancer Interdiscip Int J Am Cancer Soc 115(21):5007–5017
4. Oken MM, Hocking WG, Kvale P, Andriole GL, Buys SS, Church TR, Crawford ED, Fouad MN, Isaacs C, Reding DJ, Weissfeld JL (2011) Screening by chest radiograph and lung cancer mortality: the prostate, lung, colorectal, and ovarian (PLCO) randomized trial. JAMA 306(17):1865–1873
5. National Lung Screening Trial Research Team (2011) Reduced lung-cancer mortality with low-dose computed tomographic screening. N Engl J Med 365(5):395–409
6. Suzuki K, Kusumoto M, Watanabe SI, Tsuchiya R, Asamura H (2006) Radiologic classification of small adenocarcinoma of the lung: radiologic-pathologic correlation and its prognostic impact. Ann Thorac Surg 81(2):413–419
7. Xu Y, Wang Y, Razmjooy N (2022) Lung cancer diagnosis in CT images based on alexnet optimized by modified bowerbird optimization algorithm. Biomed Signal Process Control 77:103791
8. Cai W, Mohammaditab R, Fathi G, Wakil K, Ebadi AG, Ghadimi N (2019) Optimal bidding and offering strategies of compressed air energy storage: a hybrid robust-stochastic approach. Renew Energy 143:1–8
9. Abdullah MF, Sulaiman SN, Osman MK, Karim NKA, Shuaib IL, Alhamdu MDI (2020) Classification of lung cancer stages from CT scan images using image processing and k-Nearest neighbours. In: 2020 11th IEEE Control and System Graduate Research Colloquium (ICSGRC), p 68–72. IEEE
10. Dandıl E, Çakiroğlu M, Ekşi Z, Özkan M, Kurt ÖK, Canan A (2014) Artificial neural network-based classification system for lung nodules on computed tomography scans. In: 6th International conference of soft computing and pattern recognition (SoCPaR) p 382–38. IEEE
11. Diaz JM, Pinon RC, Solano G (2014) Lung cancer classification using genetic algorithm to optimize prediction models. In: IISA 2014, The 5th International Conference on Information, Intelligence, Systems and Applications. p 1–6. IEEE
12. Zheng S, Guo J, Cui X, Veldhuis RN (2019) Automatic pulmonary nodule detection in CT scans using convolutional neural

networks based on maximum intensity projection. IEEE Trans Med Imaging 39:797–805
13. Kareem HF, Al-Husieny MS, Mohsen FY, Khalil EA, Hassan ZS (2021) Evaluation of SVM performance in the detection of lung cancer in marked CT scan dataset. Indones J Electr Eng Comput Sci 21(3):1731
14. Al-Yasriy HF, Al-Husieny MS, Mohsen FY, Khalil EA, Hassan ZS (2020) Diagnosis of lung cancer based on CT scans using CNN. In IOP Conference Series: Materials Science and Engineering Vol. 928, No. 2, p 022035. IOP Publishing
15. Roy TS, Sirohi N, Patle A (2015) Classification of lung image and nodule detection using fuzzy inference system. In: International conference on computing, communication & automation, p 1204–1207. IEEE
16. Zhang F, Wang Q, Li H (2020) Automatic segmentation of the gross target volume in non-small cell lung cancer using a modified version of ResNet. Technol Cancer Res Treat 19:1533033820947484
17. Nakrani MG, Sable GS, Shinde UB (2020) ResNet based lung nodules detection from computed tomography images. Int J Innov Technol Exploring Eng 1711–4
18. Zhang Y, Feng W, Wu Z, Li W, Tao L, Liu X, Zhang F, Gao Y, Huang J, Guo X (2023) Deep-learning model of ResNet combined with CBAM for malignant–benign pulmonary nodules classification on computed tomography images. Medicina 59(6):1088
19. Xie Y, Xia Y, Zhang J, Song Y, Feng D, Fulham M, Cai W (2018) Knowledge-based collaborative deep learning for benign-malignant lung nodule classification on chest CT. IEEE Trans Med Imaging 38(4):991–1004
20. Xie Y, Zhang J, Xia Y, Fulham M, Zhang Y (2018) Fusing texture, shape and deep model-learned information at decision level for automated classification of lung nodules on chest CT. Inf Fusion 42:102–110
21. Rajasekar V, Vaishnnave MP, Premkumar S, Sarveshwaran V, Rangaraaj V (2023) Lung cancer disease prediction with CT scan and histopathological images feature analysis using deep learning techniques. Results Eng 18:101111
22. Mhaske D, Rajeswari K, Tekade R (2019) Deep learning algorithm for classification and prediction of lung cancer using CT scan images. In: 2019 5th International Conference On Computing, Communication, Control And Automation (ICCUBEA). p 1–5. IEEE
23. Lakshmanaprabu SK, Mohanty SN, Shankar K, Arunkumar N, Ramirez G (2019) Optimal deep learning model for classification of lung cancer on CT images. Futur Gener Comput Syst 92:374–382
24. Sajja TK, Devarapalli RM, Kalluri HK (2019) Lung cancer detection based on CT scan images by using deep transfer learning. Traitement du Signal 36(4):339–344
25. Nigudgi S, Bhyri C (2023) Lung cancer CT image classification using hybrid-SVM transfer learning approach. Soft Comput 27(14):9845–9859
26. Wang S, Dong L, Wang X, Wang X (2020) Classification of pathological types of lung cancer from CT images by deep residual neural networks with transfer learning strategy. Open Med 15(1):190–197
27. Heidari A, Javaheri D, Toumaj S, Navimipour NJ, Rezaei M, Unal M (2023) A new lung cancer detection method based on the chest CT images using federated learning and blockchain systems. Artif Intell Med 141:102572
28. Adnan M, Kalra S, Cresswell JC, Taylor GW, Tizhoosh HR (2022) Federated learning and differential privacy for medical image analysis. Sci Rep 12(1):1953
29. Nazir S, Kaleem M (2023) Federated learning for medical image analysis with deep neural networks. Diagnostics 13(9):1532
30. Al-Huseiny MS, Sajit AS (2021) Transfer learning with GoogLeNet for detection of lung cancer. Indones J Electr Eng Comput Sci 22(2):1078–1086
31. Solyman S, Schwenker F (2022) Lung tumor detection and recognition using deep convolutional neural networks. In: Pan African Conference on Artificial Intelligence. Cham: Springer Nature Switzerland, p 79–91
32. Abdollahi J (2023) Evaluating LeNet Algorithms in Classification Lung Cancer from Iraq-Oncology Teaching Hospital/National Center for Cancer Diseases. arXiv preprint arXiv:2305.13333
33. Al-Yasriy HF, Al-Husieny MS, Mohsen FY, Khalil EA, Hassan ZS (2020) Diagnosis of lung cancer based on CT scans using CNN. In: IOP Conference Series: Materials Science and Engineering Vol 928, No 2. IOP Publishing, p 022035
34. Promy TF, Joya NI, Turna TH, Sukhi ZN, Ashraf FB, Uddin J (2022) Cancer diseases diagnosis using deep transfer learning architectures. In: International Conference on Machine Intelligence and Emerging Technologies. Cham: Springer Nature Switzerland, p 226–237
35. He C, Annavaram M, Avestimehr S (2020) Group knowledge transfer: Federated learning of large cnns at the edge. Adv Neural Inf Process Syst 33:14068–14080
36. Geiping J, Bauermeister H, Dröge H, Moeller M (2020) Inverting gradients-how easy is it to break privacy in federated learning? Adv Neural Inf Process Syst 33:16937–16947
37. Koonce B, Koonce BE (2021) Convolutional neural networks with swift for tensorflow: Image recognition and dataset categorization. Apress, New York, NY, USA, pp 109–123
38. Li B, Lima D (2021) Facial expression recognition via ResNet-50. Int J Cogn Comput Eng 2:57–64
39. Zhou P, Feng J, Ma C, Xiong C, Hoi SCH (2020) Towards theoretically understanding why sgd generalizes better than adam in deep learning. Adv Neural Inf Process Syst 33:21285–21296
40. Keskar NS, Socher R (2017) Improving generalization performance by switching from adam to sgd. arXiv preprint arXiv:1712.07628
41. Wang J, Wiens J (2020) AdaSGD: Bridging the gap between SGD and Adam. arXiv preprint arXiv:2006.16541